

#### REMARKS

This Amendment is filed in response to the Office Action dated June 3, 2005, which has a shortened statutory period set to expire September 3, 2005. In view of the following remarks, a reconsideration of the present patent application is respectfully requested.

#### **Rejection under 35 U.S.C. §102(b)**

The Official Action rendered that Claims 1, 5-8 and 11-14 are rejected under 35 U.S.C. §102(b) as being anticipated by Shields (WO 02/11211). The Applicant respectfully traverses the pending rejection. Reconsideration of the present patent application is respectfully requested.

With regard to the present application, it should be noted that one of the main features thereof is that the existence of the insulating layer. It's known to one skilled in the art that a dark current will always occur when a bias voltage is applied to the semiconductor layer of an infrared photodetector. However, since the existence of the insulating layer 13 of the present application is used as a current block barrier, the undesired dark current can be significantly reduced accordingly.

Nevertheless, please refer to Figs. 6-9 and 13-19 of the cited Reference WO 02/11211, the quantum well layer 39 is always in contact with the first tunnel barrier layer 37 and the second tunnel barrier layer 41. In other words, the quantum well structure of the cited Reference WO 02/11211 includes the quantum well layer 39 sandwiched between the first and second tunnel barrier layers 37 and 41, i.e., the first and second tunnel barrier layers 37 and 41 could be regarded as the certain side walls of the quantum well structure. Similarly, as shown in Figs. 1-5, the first barrier layer 11 and the second barrier layer 19 are also parts of the relevant quantum well structures. Furthermore, as shown in Page 18, paragraph 2 of the cited reference WO 02/11211, the second barrier layer 19 is thin

enough so that when the first energy level 13 and the second energy level 17 align, a resonant tunneling takes place through the first barrier layer 11 and the second barrier layer 19. As above, the thickness of the barrier layer is always tried as thin as possible so as to enable the carrier to tunnel through.

In the present application, however, as described in paragraph [0026] and Fig. 1, the infrared photodetector mainly comprises a conducting layer 11, a p-type semiconductor layer 12 having five layers of Ge quantum dots, an insulating layer 13 and a voltage source 14. The semiconductor layer 12 further comprises a Si substrate 121, a Si buffer layer 122, a Ge wetting layer 123, a Ge quantum dot 124, a Si spacer layer 125 and a Si cap layer 126. As above, it's easy for one skilled in the art to understand that each quantum well structure of the present application comprises the Ge quantum dot 124 and its adjacent Si layers. In other word, only the relevant Si layers and the Ge quantum dot are parts of the quantum well structures, but the insulating layer 13 is completely independent from the "quantum well structure".

In addition, as shown in Fig. 5 and described in paragraph [0030] of the present application, another infrared photodetector according to a preferred embodiment of the present invention mainly comprises a silicon or silicon on insulator (SOI) substrate 51, a highly doped silicon layer 52, a semiconductor layer 53 having at least one layer of quantum well or quantum dot, an insulating layer 54, an insulating isolation layer 55, a reticular electrode 56 and an electrode 57. The insulating isolation layer 55 is used to isolate the electrode 57 and the semiconductor layer 53 having at least one layer of quantum well or quantum dot. The reticular electrode 56 can increase the irradiating area of the elements and the conducting rate of the carriers. Similarly, the so-called semiconductor layer of the present application includes the quantum well structures therein itself, and the insulating layer 54 is completely far from being relevant to a part of the quantum well structure.

As above, the quantum well layer 39, the first tunnel barrier layer 37 and the second tunnel barrier layer 41 of the cited Reference WO 02/11211 correspond to the Ge quantum dot and its relevant adjacent Si layers of the present application at most, so that it's surely unreasonable the Examiner alleges that the insulating layer of the present application (a layer between the conducting layer and the semiconductor layer having the quantum well structure therein) has been disclosed by any of layers 37, 39 or 41.

Furthermore, please refer to the recitations of independent Claims 1, 13 and 14 of the present application, it could be seen that all the claimed infrared photodectors respectively comprise a conducting layer, a semiconductor layer comprising at least one layer of quantum structure for confining a carrier in a barrier, an insulating layer and a voltage source. Moreover, paragraphs [0026], [0028] and [0030] in the present specification do support the above recitations. Therefore, since the Applicant has clearly disclosed that the quantum well structure of the present application is a part of the semiconductor layer in the independent Claims 1, 13 and 14 and the novel insulating layer is also indeed provided in the relevant recitations, Claims 1, 13 and 14 should own the patentabilities, respectively. Furthermore, since independent Claims 1, 13 and 14 have the patentabilities, their dependent claims should also be patentable as being dependent on the allowable Claims 1, 13 and 14.

Moreover, please be advised that the present application relates to a novel metal-insulator-semiconductor (MIS) Ge-Si quantum-dot infrared photodetectors (QDIPs), but the conventional device relates to the metal-semiconductor-metal structure. In addition, it should be noted that, as described in the last sentence of the INTRODUCTION of the Attachment (B. C. Hsu et al., 2004, Novel MIS Ge-Si Quantum-Dot Infrared Photodetectors, IEEE Electron Device Letters, Vol. 25, No. 8, pp. 544-546) published by the inventors of the present application, the undesired dark current can be significantly reduced due to the existence of the insulating layer.

As above, since the present application does disclose a new concept of providing an insulating layer between the electrode layer and the semiconductor layer, and the relevant research paper has been accepted by the professional in this art, there is no room to doubt the progressiveness, novelty and utility of the present application.

#### **Rejection under 35 U.S.C. §103(a)**

The Official Action rendered that Claim 2 is rejected under 35 U.S.C. §103(a) as being unpatentable over Shields (WO 02/11211) in view of Thomas et al., (JP2002198503A). In addition, the Official Action also rendered that Claims 3-4 are rejected under 35 U.S.C. §103(a) as being unpatentable over Shields (WO 02/11211) in view of Akama (US 5,679,690). Furthermore, the Official Action also rendered that Claim 9 is rejected under 35 U.S.C. §103(a) as being unpatentable over Shields (WO 02/11211) in view of Kibbel et al. (US 2002/0112755). Moreover, the Official Action also rendered that Claim 10 is rejected under 35 U.S.C. §103(a) as being unpatentable over Shields (WO 02/11211) in view of Berger et al. (US 2003/0049894). The Applicant respectfully disagrees. A reconsideration of the present patent application is respectfully requested.

As above, since the present application discloses a new concept of providing an insulating layer between the electrode layer and the semiconductor layer and none of the cited References (WO 02/11211, JP2002198503A, US 5,679,690, US 2002/011275 and US 2003/0049894) can imply, teach or suggest the above concept, the present invention cannot be anticipated by them and further cannot be achieved by one skilled in the art from the teachings thereof.

Accordingly, Claims in the present invention are patentable over the cited references WO 02/11211, JP2002198503A, US 5,679,690, US 2002/011275 and US 2003/0049894.

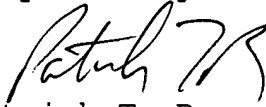
As above-mentioned, it is clear that the present application does own the features patentably distinguishing over those in the cited References and, undoubtedly, the cited References fail to disclose or teach the details of the infrared photodectors as recited in the present application. So that, the present application is creative over the prior art. As set forth in the above discussions, it's clear that the present application is patentable.

CONCLUSION

Claims 1-14 are pending in the present Application. Reconsideration and allowance of these claims is respectfully requested.

If there are any questions, please telephone the undersigned at (408) 451-5902 to expedite prosecution of this case.

Respectfully submitted,



Customer No.: 022888

Patrick T. Bever  
Attorney for Applicant(s)  
Reg. No. 33,834

I hereby certify that this correspondence is being deposited with the United States Postal Service as FIRST CLASS MAIL in an envelope addressed to: Mail Stop Amendment, Commissioner for Patents, P.O. Box 1450, Alexandria, VA 22313-1450 on August 30, 2005.

<u>8/30/05</u>	<u>Rebecca A. Baumann</u>
Date	Signature: Rebecca A. Baumann

# Novel MIS Ge-Si Quantum-Dot Infrared Photodetectors

B.-C. Hsu, *Student Member, IEEE*, C.-H. Lin, P.-S. Kuo, S. T. Chang, *Member, IEEE*, P. S. Chen, C. W. Liu, *Senior Member, IEEE*, J.-H. Lu, and C. H. Kuan, *Member, IEEE*

**Abstract**—The metal-insulator-semiconductor (MIS) Ge-Si quantum-dot infrared photodetectors (QDIPs) are successfully demonstrated. Using oxynitride as gate dielectric instead of oxide, the operating temperature reaches 140 and 200 K for 3–10 and 2–3  $\mu\text{m}$  detection, respectively. From the photoluminescence spectrum, the quantum-dot structures are responsible for the 2–3  $\mu\text{m}$  response with high operation temperature, and the wetting layer structures may be responsible for the 3–10  $\mu\text{m}$  response. This novel MIS Ge/Si QDIP can increase the functionality of Si chip such as noncontact temperature sensing and is compatible with ultra-large scale integration technology.

**Index Terms**—Ge, metal-insulator-semiconductor (MIS), oxynitride, quantum-dot infrared photodetectors (QDIPs), quantum-dot.

## I. INTRODUCTION

**D**UE TO THE low dark current, high operation temperature, and normal incident detection, the quantum-dot infrared photodetector (QDIP) is very attractive in military, medical, astronomical, and other applications. The most common material systems used for the QDIPs are III-V-based systems. The QDIP with the self-assembled InGaAs quantum-dots has been demonstrated with 3.25 mA/W responsivity at 60 K, with the wavelength of 9.2  $\mu\text{m}$  [1]. Tang *et al.* also demonstrated the ten stack InAs-GaAs QDIP at 2.5–7  $\mu\text{m}$  with  $2.4 \times 10^8 \text{ cm}^2/\text{Hz}^{1/2}/\text{W}$  detectivity at 250 K [2]. The III-V-based QDIP has reached an operation temperature of 260 K using the InGaAs-GaAs quantum-dots due to the low dark current and long carrier lifetime in the quantum-dots [3].

Due to the compatibility with Si ultra-large scale integration (ULSI) process and the tremendous capability of digital signal process on Si chip, the Si-SiGe heterojunction photodetectors are desired to have the infrared detection wavelengths beyond 1.1  $\mu\text{m}$ . The metal-insulator-semiconductor (MIS) Ge quantum-dot photodetector have been reported with 1.3 and 1.5

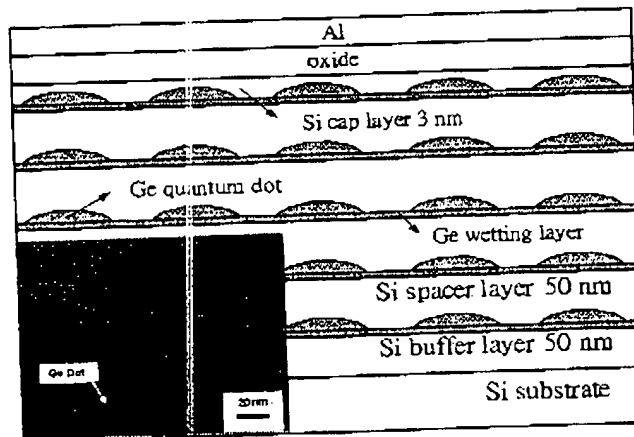


Fig. 1. Structure of the MIS Ge-Si QDIP. The five-layer Ge quantum-dots were prepared by ultrahigh-vacuum chemical vapor deposition, and the inset shows the TEM micrograph of the self-assembled Ge dots.

$\mu\text{m}$  responses [4]. In this letter, the MIS Ge-Si QDIP is demonstrated using the hole subband transitions of the quantum-dot and wetting layers. By using the tunneling junction in the MIS structure as a current blocking barrier, the dark current is reduced as compared to the metal-semiconductor-metal (MSM) devices [2], [3].

## II. DEVICE FABRICATION

The schematic structure of the MIS Ge-Si QDIP is illustrated in Fig. 1 and the transmission electron microscopy (TEM) image of the Ge quantum-dot is shown in the inset. After an Si buffer layer of 50 nm, five periods of self-assembled Ge-Si quantum-dots were grown on a p-type Si substrate at 600  $^{\circ}\text{C}$  under the Stranski-Krastanov (SK) growth mode [5]. Silane ( $\text{SiH}_4$ ) and germane ( $\text{GeH}_4$ ) were used as the Si and Ge precursor, respectively. To separate the Ge layers, a 50-nm Si spacer layer was used and a 3-nm Si cap was deposited as a top layer for the subsequent dielectric growth. The base width and height of the Ge dots are  $\sim 100$  and  $\sim 7$  nm, respectively. The Ge dot density is  $\sim 10^{10} \text{ cm}^{-2}$ , measured on the sample with the same growth condition without the Si cap. All layers were unintentionally doped with an estimated hole concentration  $\sim 1 \times 10^{16} \text{ cm}^{-3}$ .

The MIS QDIPs had Al gate electrodes with various circular areas defined by photolithography. To avoid strain relaxation and Ge segregation, low-temperature liquid phase deposition (LPD) process was used to deposit the gate oxide with the advantages of low cost, selective growth, and high throughput [6].

Manuscript received February 25, 2004. This work was supported by the National Science Council, Taiwan, R.O.C., under Contracts 92-2120-E-002-006 and 92-2215-E-002-007. The review of this letter was arranged by Editor P. Yu. B.-C. Hsu, C.-H. Lin, P.-S. Kuo, J.-H. Lu, and C. H. Kuan are with the Department of Electrical Engineering and Graduate Institute of Electronics Engineering, National Taiwan University, Taipei, Taiwan, R.O.C. S. T. Chang is with the Department of Electronic Engineering, Chung Yuan Christian University, Chung-Li, Taiwan, R.O.C. P. S. Chen is with the ERSO/ITRI, Hsinchu, Taiwan, R.O.C. (e-mail: chcc@cc.ee.ntu.edu.tw).

C. W. Liu is with the Department of Electrical Engineering and Graduate Institute of Electronics Engineering, National Taiwan University, Taipei, Taiwan, R.O.C., and also with the ERSO/ITRI, Hsinchu, Taiwan, R.O.C. Digital Object Identifier 10.1109/LED.2004.831969

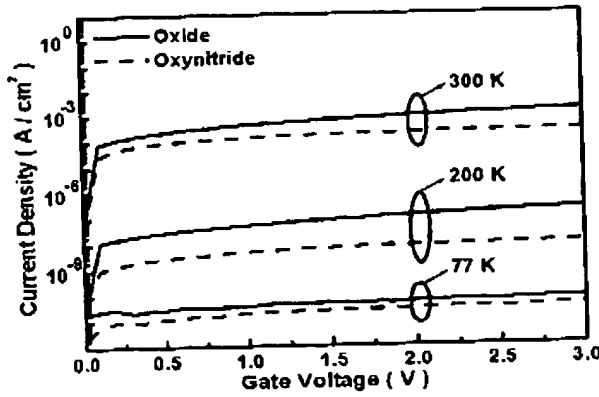


Fig. 2. Dark current of MIS Ge/Si QDIPs with LPD oxide and oxynitride at different temperature. The device with oxynitride has lower dark current density.

Details can be found in the [6]. To further reduce the dark current,  $\text{NH}_4\text{OH}$  was added into the saturated solution during LPD process to form the  $\text{SiON}$  film [7].

### III. RESULTS AND DISCUSSION

Fig. 2 shows the current-voltage ( $I$ - $V$ ) characteristics at different temperature for the devices with oxide or oxynitride as gate dielectrics. The thicknesses of the LPD oxide and oxynitride were  $\sim 1.5$  nm. The dark current of MIS tunneling diode is dominated by thermal generation of electron-hole pairs through the defects in the depletion region and at the  $\text{Si-SiO}_2$  interface [8]. The LPD oxynitride has a low interface state density, and thus, has a low dark current as compared to LPD oxide. For an n-channel MIS (NMIS) Ge QDIP under inversion bias, the thermally generated electrons tunnel through the insulator layer, and the holes thermally generated in the deep depletion region as well as the holes tunneling from the gate electrode are swept toward the Si substrate. The Ge quantum-dots are placed in the depletion region at inversion bias to have sufficient electrical field to drift the photo-excited holes.

The spectral responsivity of the NMIS Ge/Si QDIP with oxynitride is illustrated in Fig. 3. The infrared is normal incident to the device without any polarization. For p-type quantum wells, the optical selection rules do allow both normal and parallel incident absorption. The normal incident absorption of p-type Si-SiGe quantum wells are also reported in the previous studies [9], [10]. The spectral responsivity is calibrated with a blackbody radiation source [2]. The spectral dependence of the responsivity is measured by Fourier transform infrared (FTIR) spectrometer (Perkin-Elmer Spectrum 2000). Note that the measured spectrum is the multiplication of the light source spectrum, and the spectral response of the detector. The device spectral response is obtained after the correction of light source spectral dependence. The spectrum can be divided into two absorption regions (2–3, and 3–10  $\mu\text{m}$ ). For 3–10  $\mu\text{m}$  detection, the peak wavelength is located at 6.8  $\mu\text{m}$  and the maximum operating temperature is about 140 K. For 2–3  $\mu\text{m}$  detection, the peak wavelength is located at 2.7  $\mu\text{m}$  and the operating temperature is up to 200 K (Fig. 3). At low temperature, the responsivity increases with the increasing

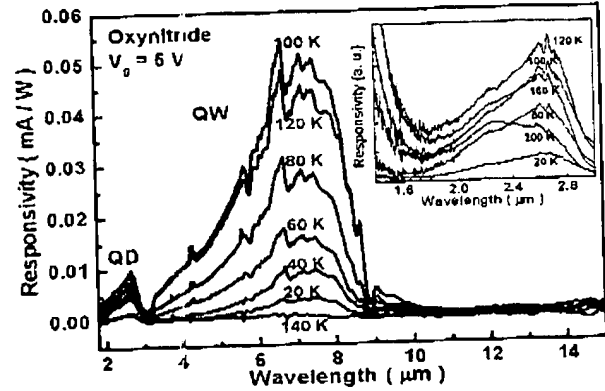


Fig. 3. Spectral responsivity of the device with oxynitride at different temperature. The operating temperature is 140 K for 3–10  $\mu\text{m}$  detection. The inset shows the 2–3  $\mu\text{m}$  response and the operating temperature reaches 200 K.

temperature due to the increasing thermal energy of confined holes in the quantum-dots and quantum wells. With higher thermal energy, more holes can relaxed to the bottom electrode without being trapped by quantum-dots after photon excitation. After  $\sim 100$  K, the second bound state is more populated with holes, less holes are in the ground state, the bound-to-bound transition also becomes difficult. Therefore, the responsivity drops as the temperature further increases. Note that the strong spectral response for wavelengths smaller than 1.7  $\mu\text{m}$  is due to the interband transition of the Si-Ge quantum-dots.

Since the operating temperature is higher for 2–3  $\mu\text{m}$  detection, this short wavelength response probably comes from the quantum-dot structure due to the better quantum confinement, while the 3–10  $\mu\text{m}$  response may be dominated by the wetting layer structure. By assuming the Ge dot is a simple box of infinite barrier, the allowed energies in the dot can be evaluated as [11]

$$E_{n,k,l} = \frac{\pi^2 \hbar^2}{2m^*} \left( \frac{n^2}{L_x^2} + \frac{k^2}{L_y^2} + \frac{l^2}{L_z^2} \right) \quad n, k, l = 1, 2, 3 \dots (1)$$

where  $m^*$  is the Ge heavy hole effective mass equal to  $0.3 m_0$ ,  $L_x$  and  $L_y$  are dot base widths, and  $L_z$  is the dot height.  $L_z$  is  $\sim 7$  nm in our sample, while  $L_x$  is 4–4.5 nm in [11]. The ground state energy of the heavy hole is  $\sim 100$  meV. Fig. 4 shows the 20 K photoluminescence (PL) spectrum of the multilayer Ge quantum-dots structure. The Si bandgap at 20 K is about 1.17 eV. The PL spectrum indicates that the short wavelength response comes from the quantum-dot structure for the bound-to-continuum transition ( $\sim 0.4$  eV) [12]. With the ground state energy of  $\sim 100$  meV, the valence band offset between Si and Ge dots is  $\sim 0.5$  eV. Note that the bandedge of the bound state is estimated as the cutoff energy at the low-energy side of the PL line in Fig. 4.

The device detectivity at 100 K reaches  $10^{10}$  and  $10^9 \text{ cm-Hz}^{1/2}/\text{W}$  for 6.8  $\mu\text{m}$  and 2.7  $\mu\text{m}$ , respectively. The normalized detectivity  $D^*$  is defined as

$$D^* = \frac{\sqrt{A \Delta f}}{NEP} = \frac{\sqrt{A \Delta f}}{I_R} \quad (2)$$



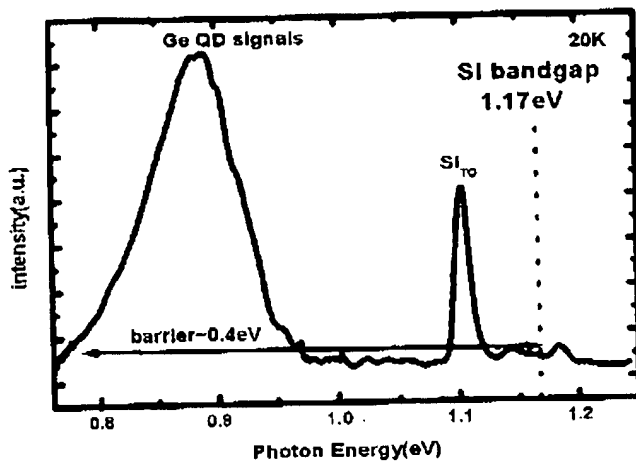


Fig. 4. The 20 K PL spectrum for a multilayer Ge-Si quantum-dot structure. Si bandgap is  $\sim 1.17$  eV at 20 K, and the QD barrier is  $\sim 0.4$  eV.

where  $A$  is the detector area,  $\Delta f$  is the equivalent bandwidth of the electronic system, and  $NEP = i_n/R$  is the noise equivalent power. The  $i_n$  is current noise and  $R$  is the responsivity. The current noise is limited by the dark current and can be approximated as the shot noise  $(2eI_d\Delta f)^{1/2}$ , where  $I_d$  is the measured dark current. Due to the low dark current, the peak detectivity is relatively large. Due to the larger dark current of the device with LPD oxide, the operating temperature of the LPD oxide device is only 80 K for 3–10  $\mu\text{m}$  detection and is 120 K for 2–3  $\mu\text{m}$  detection. Note that there is no electron-hole pair generation through interface states under the infrared exposure, since the similar spectrum was observed for the Schottky contact MSM detectors [13].

#### IV. CONCLUSION

The MIS Ge-Si QDIPs using hole subband transitions are successfully demonstrated. The maximum operating temperature is 140 K for 3–10  $\mu\text{m}$  and is up to 200 K for 2–3  $\mu\text{m}$  detection using LPD oxynitride as gate dielectrics. Under infrared exposures, the holes confined in the quantum-dots may

have bound-to-continuum and bound-to-bound transitions, responsible for the 2–3 and 3–10  $\mu\text{m}$  responses, respectively. The device peak detectivity is  $10^{10}$  and  $10^9$   $\text{cm}\cdot\text{Hz}^{1/2}/\text{W}$  for 6.8  $\mu\text{m}$  and 2.7  $\mu\text{m}$ , respectively.

#### REFERENCES

- [1] S. J. Xu, S. J. Chua, T. Mei, X. C. Wang, X. H. Zhang, G. Karunasiri, W. J. Fan, C. H. Wang, J. Jiang, S. Wang, and X. G. Xie, "Characteristics of InGaAs quantum-dot infrared photodetectors," *Appl. Phys. Lett.*, vol. 73, pp. 3153–3155, 1998.
- [2] S.-F. Tang, S.-Y. Lin, S.-C. Lee, and C. H. Kuan, "High temperature operated ( $\sim 250$  K) photovoltaic-photoconductive (PV-PC) mixed-mode InAs/GaAs quantum-dot infrared photodetector," in *IEDM Tech. Dig.*, 2000, pp. 597–600.
- [3] L. Jiang, S. S. Li, C. E. Ross, and K. S. Jones, "In<sub>0.4</sub>Ga<sub>0.6</sub>As-GaAs quantum-dot infrared photodetector with operating temperature up to 260 K," *Appl. Phys. Lett.*, vol. 82, pp. 1986–1988, 2003.
- [4] B.-C. Hsu, S. T. Chang, C.-R. Shie, C.-C. Lai, P. S. Chen, and C. W. Liu, "High efficient 820 nm MOS Ge quantum-dot photodetectors for short reach integrated optical receivers," in *IEDM Tech. Dig.*, 2002, pp. 91–94.
- [5] T. I. Kamins, L. A. A. Ohlberg, R. S. Williams, W. Zhang, and S. Y. Chou, "Positioning of self-assembled, single-crystal, germanium islands by silicon nanoimprinting," *Appl. Phys. Lett.*, vol. 74, pp. 1773–1775, 1999.
- [6] B.-C. Hsu, W.-C. Hua, C.-R. Shie, K.-F. Chen, and C. W. Liu, "The growth and electrical characteristics of liquid phase deposition SiO<sub>2</sub> on Ge," *IEEE Electrochem. Solid-State Lett.*, vol. 6, pp. F9–F11, Feb. 2003.
- [7] M.-K. Lee, S.-Y. Lin, and J.-M. Shyr, "Characteristics of oxynitride prepared by liquid phase deposition," *J. Electrochem. Soc.*, vol. 148, no. 1, pp. F1–F4, 2001.
- [8] C.-H. Lin, B.-C. Hsu, M. H. Lee, and C. W. Liu, "A comprehensive study of gate inversion current of metal-oxide-silicon tunneling diodes," *IEEE Trans. Electron Devices*, vol. 48, pp. 2125–2130, Dec. 2001.
- [9] J. S. Park, R. P. G. Karunasiri, and K. L. Wang, "Intervalence-subband transition in Si/Ge/Si multiple quantum wells-normal incident detection," *Appl. Phys. Lett.*, vol. 61, pp. 681–683, 1992.
- [10] D. E. Weeks, S. H. Yang, M. R. Gregg, S. J. Novotny, K. D. Greene, and R. L. Henghold, "Intersubband infrared absorption spectra of Si/Si<sub>1-x</sub>Ge<sub>x</sub> quantum wells grown in the [110] direction," *Phys. Rev. B, Condens. Matter*, vol. 65, pp. 195314–1–9, 2002.
- [11] J. L. Liu, W. G. Wu, A. Balandin, G. L. Jin, and K. L. Wang, "Intersubband absorption in boron-doped multiple Ge quantum-dots," *Appl. Phys. Lett.*, vol. 74, pp. 185–187, 1999.
- [12] V. L. Thanh, V. Yam, L. H. Nguyen, Y. Zheng, P. Boucaud, D. Débarre, and D. Bouchier, "Vertical ordering in multilayers of self-assembled Ge/Si(001) quantum-dots," *J. Vac. Sci. Technol. B, Microelectron. Process. Phenom.*, vol. 20, no. 3, pp. 1259–1265, 2002.
- [13] Y. H. Peng, J.-H. Lu, C. H. Kuan, C. W. Liu, P.-S. Chen, Z. Pei, M.-J. Tsai, S. W. Lee, L. J. Chen, M. H. Ya, and Y. P. Chen, "Schottky quantum-dots infrared photodetector with far infrared response," in *Proc. ISTDM*, 2003, pp. 219–220.